PROCEEDINGS OF SPIE

SPIEDigitalLibrary.org/conference-proceedings-of-spie

Experimental validation of tunable features in laser-induced plasma resonators

Colón Quiñones, Roberto, Cappelli, Mark

Roberto A. Colón Quiñones, Mark A. Cappelli, "Experimental validation of tunable features in laser-induced plasma resonators," Proc. SPIE 10343, Metamaterials, Metadevices, and Metasystems 2017, 103430B (24 August 2017); doi: 10.1117/12.2276971

SPIE.

Event: SPIE Nanoscience + Engineering, 2017, San Diego, California, United States

Experimental validation of tunable features in laser-induced plasma resonators

Roberto A. Colón Quiñones and Mark A. Cappelli

Stanford University, Stanford, CA, USA

ABSTRACT

Measurements are presented which examine the use of gaseous plasma elements as highly-tunable resonators. The resonator considered here is a laser-induced plasma kernel generated by focusing the fundamental output from a Q-switched Nd:YAG laser through a lens and into a gas at constant pressure. The near-ellipsoidal plasma element interacts with incoming microwave radiation through excitation of low-order, electric-dipole resonances similar to those seen in metallic spheres. The tunability of these elements stems from the dispersive nature of plasmas arising from their variable electron density, electron momentum transfer collision frequency, and the concomitant effect of these properties on the excited surface plasmon resonance. Experiments were carried out in the Ku band of the microwave spectrum to characterize the scattering properties of these resonators for different values of electron density. The experimental results are compared with results from theoretical approximations and finite element method electromagnetic simulations. The described tunable resonators have the potential to be used as the building blocks in a new class of all-plasma metamaterials with fully three-dimensional structural flexibility.

Keywords: laser, plasma, gas, resonator, metamaterial, active, tunable, reconfigurable

1. INTRODUCTION

The electromagnetic (EM) properties of most natural materials are dictated by the resonances of their constituent atoms, which are typically ~ 1 angstrom in size. Because of the small spacing between these atoms, many EM wavelengths of engineering interest (vacuum ultraviolet waves or longer) only probe their average or effective properties. A metamaterial (MTM), i.e., an artificial material engineered to exhibit EM properties not readily found in nature, follows the same principle. The resonantly active elements in MTMs and their relative spacing are designed to create an effectively homogenous medium with engineered EM properties. Such a medium is achieved when the spacing between the constituent elements is smaller than a quarter of the guided wavelength ($p < \lambda_0/4$).[1] The ability to create MTMs with exotic effective properties such as artificial magnetism, negative refraction, and perfect lensing, has generated much interest during the last few decades.[2]

In recent years, efforts have focused on exploring the tunability of these properties. Tunable MTM devices have exploited the electro-optical, liquid-crystal, phase-change, and superconducting response of their constituent elements.[3] One class of potentially tunable elements that has been largely overlooked are gaseous plasmas, which can be incorporated into more commonly-used MTMs to form composite periodic structures with tunable features.[4] The tunability of these structures stems from the dispersive nature of plasmas arising from their variable electron density (n_e) and electron momentum transfer collision frequency (γ). These two plasma properties are in turn controlled by the energy invested by the ionizing source and the pressure/composition of the gas.

The majority of past research related to plasma MTMs has mainly focused on the development of composites that integrate plasmas into conventional metallic resonant structures[5–10] or into novel dielectric resonator arrays.[11] This paper reports on the potential to achieve a MTM composed entirely of plasmas. Specifically, this study describes the EM properties of a laser-induced plasma resonator, which is generated by focusing the fundamental output from a Q-switched Nd:YAG laser through a lens and into a gas at constant pressure (Fig. 1a).

Further author information: (Send correspondence to R.A.C.Q.)
R.A.C.Q.: E-mail: racolon@stanford.edu
M.A.C.: E-mail: cap@stanford.edu

Metamaterials, Metadevices, and Metasystems 2017, edited by Nader Engheta, Mikhail A. Noginov, Nikolay I. Zheludev, Proc. of SPIE Vol. 10343, 103430B
 · doi: 10.1117/12.2276971

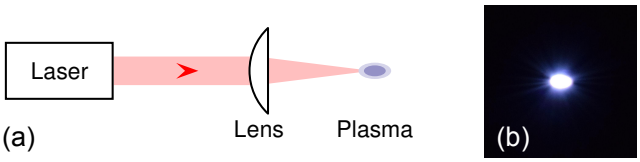

Figure 1. (a) Schematic of experimental setup used to generate a laser-induced plasma. (b) Optical image of laser-induced plasma in air at atmospheric pressure.

The near-ellipsoidal[12] plasma resonator (Fig. 1b) interacts with incoming microwave radiation through excitation of low-order, electric-dipole resonances similar to those seen in metallic spheres.[13] For frequencies below the plasma frequency (ω_p), the collective scattering response of a MTM composed entirely of these plasmonic resonators results in a region of negative effective dielectric constant centered at the frequency of the excited surface mode.[14] Potential applications of such MTMs include, but are not limited to, highly-tunable reflective surfaces and negative-index mediums with fully three-dimensional structural flexibility.

In this paper, a theoretical estimate of the resonance frequency of these elements is obtained through an electrostatic approximation of the polarizability of the plasma ellipsoids. In order to determine the approximation's degree of accuracy, these results are then compared to results obtained from finite element method (FEM) simulations. To conclude, the results of single-particle scattering experiments are also presented, which provide a qualitative validation of the existence of the surface modes predicted by the aforementioned methods.

2. RESULTS

2.1 Theoretical Approximations

An exact solution for the scattering fields from an ellipsoid, similar to the solution derived by G. Mie for the scattering fields from a sphere,[15] does not exist. However, for sub-wavelength particles, an electrostatic approximation can be used to obtain an approximate solution. Through such an approach, the polarizability of an ellipsoid in a field parallel to one of its principal axes can be defined as[13]

$$\alpha = v\frac{\epsilon - 1}{1 + L(\epsilon - 1)}, \tag{1}$$

where v is the volume of the ellipsoid, L is a geometrical factor dependent on the eccentricity and orientation of the ellipsoid, and ϵ is the dielectric constant of the plasma ellipsoid, which was defined by a Drude model as

$$\epsilon = 1 - \frac{\omega_p^2}{\omega^2 + i\gamma\omega}; \quad \omega_p = \sqrt{\frac{n_e e^2}{m_e \epsilon_0}}, \tag{2}$$

where e is the electron charge, m_e is the electron mass, and ϵ_0 is the free space permittivity. The absorption and scattering cross sections of such ellipsoids can then be written in terms of the polarizability as[13]

$$C_{\text{abs}} = k\text{Im}\{\alpha\}; \quad C_{\text{sca}} = \frac{k^4}{6\pi}|\alpha|^2, \tag{3}$$

where k is the wave number. These cross sections quantify the amount of electromagnetic radiation that is absorbed/scattered by the ellipsoids as a function of frequency. From Eq. (3), it is possible to see that there will be a resonance (i.e. a surface mode will be excited) in both cross sections at the frequency that makes the denominator of α vanish. By setting the denominator of Eq. (1) to zero, the resonance frequency of the ellipsoid was found to be

$$\omega_0 = -\frac{i}{2}\left(\gamma + \sqrt{\gamma^2 - 4L\omega_p^2}\right) \tag{4}$$

or $\omega_0 = \omega_p\sqrt{L}$ for a collision-less ($\gamma = 0$) plasma. Eq. (4) highlights the tunable nature of the described gaseous plasma resonators. The dependence of ω_0 on ω_p and γ, confirms its dependence on the energy invested by the ionizing source and the pressure/composition of the gas, respectively. The geometrical factor, L, is independent

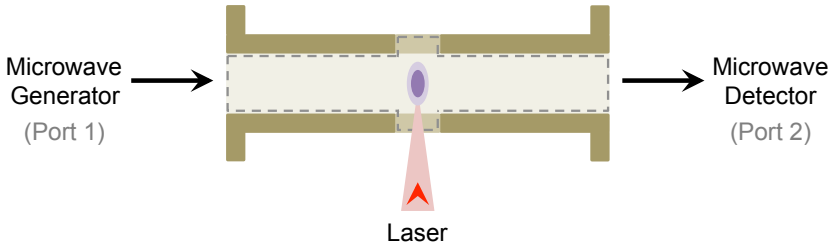

Figure 2. Schematic of experimental setup for plasma resonator scattering measurements. Simulation space is defined by gray dashed line.

of the plasma properties, but for the prolate-spheroid-like plasma generated by a laser focused to a circular beam waist,[12] it could take on two different values depending on whether the electric field is incident parallel or perpendicular to the major axis of the spheroid. The geometrical factors for the two different cases are defined as[13]

$$L_{\parallel} = \frac{1-e^2}{e^2}\left(-1+\frac{1}{2e}\ln\frac{1+e}{1-e}\right); \tag{5}$$

$$L_{\perp} = \frac{1}{4e^3}\left[2e+(e^2-1)\ln\left(\frac{1+e}{1-e}\right)\right], \tag{6}$$

where e is the eccentricity of the prolate spheroid. By substituting Eqs. (2) and (5) into Eq. (4), the resonance frequency for a plasma spheroid with major axis oriented parallel to the incident field and with properties similar to those achieved in the lab ($e = 0.866$, $n_e = 2\times10^{19}$ m^{-3}, $\gamma = 1$ GHz), was found to be $\omega_0 = 16.7 - 0.5$i GHz. Since at the given conditions $\gamma/\omega_p \ll 1$, $\mathrm{Re}(\omega_0) = 16.7$ GHz is an appropriate estimate of the resonance frequency of the described plasma spheroid. In this calculation, the eccentricity was based on spheroid dimensions (major axis: ∼4 mm, minor axis: ∼2 mm) obtained from optical images of the laser-induced plasma generated in the experiments discussed in Sec. 2.3. The plasma density and collision frequency were based on the plasma properties used in the simulations discussed in Sec. 2.2.

2.2 FEM Simulations

Simulations of a prolate plasma spheroid inside a WR62 waveguide were conducted to determine the spheroid's resonance and compare it to the value obtained through the theoretical approximations on Sec. 2.1. A schematic of a 2D cross section of the simulation space can be found on Fig. 2. The simulation space was designed to replicate the experimental setup used to generate the results discussed on Sec. 2.3. The two 4 mm diameter holes present at the top and bottom of the waveguide represent ports through which laser light comes into the waveguide and generates the plasma. All four internal walls of the waveguide were assigned perfect electric conductor (PEC) boundaries except at the laser ports where perfectly matched layer (PML) boundaries were used. A Drude model was used to model the permittivity of the plasma using the same plasma properties and geometry used for the calculation of ω_0 in Sec. 2.1. The simulation was also conducted for a range of plasma densities to illustrate the dependence of ω_0 on n_e.

A plot of the forward transmission coefficient (S_{21}) obtained from this two-port waveguide simulation can be found on Fig. 3a. As expected, for the case of $n_e = 2\times10^{19}$ m^{-3}, the resonance frequency ($\omega_0 \approx 15.2$ GHz), or frequency of least transmission, does not match exactly the resonance frequency calculated through the electrostatic approach ($\omega_0 \approx 16.7$ GHz). However, the simulation shows that the electrostatic approximation was off by less than 2 GHz and that it serves as a good estimate of the plasma spheroid's resonance. Fig. 3a also shows that ω_0 increases with n_e, providing further evidence of the tunable properties of these plasma resonators. Fig. 3b illustrates this further by showing how the transmission at a fixed frequency ($\omega = 15.2$ GHz) varies with n_e, reaching a minimum at the resonance condition of $n_e = 2\times10^{19}$ m^{-3}.

2.3 Scattering Experiments

Experiments were carried out to validate the simulations presented in Sec. 2.2. A schematic of the experimental setup can be found on Fig. 2. The experiments were carried out at a relatively low pressure of 10 Torr to

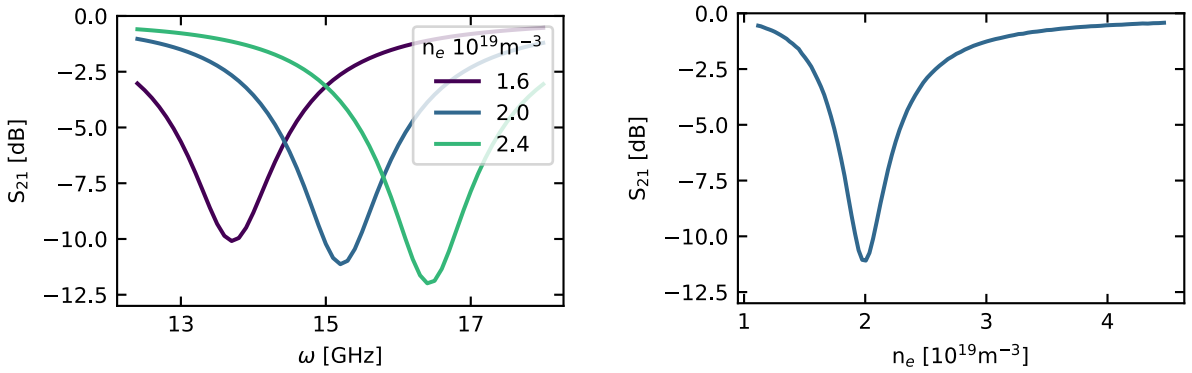

Figure 3. (a) Transmission coefficient vs. frequency for varying plasma density (simulations). (b) Transmission coefficient vs. plasma density at $\omega = 15.2$ GHz (simulations).

minimize losses associated with electron-neutral collisions in the plasma. A collimated IR beam generated by a Q-switched Nd:YAG laser (emission wavelength: 1064 nm, output energy: ∼400 mJ/p, repetition rate: 10 Hz, pulse duration: ∼10 ns, beam diameter: ∼10 mm) was used to produce the plasma. Due to the pulsed nature of this laser, the value of n_e in this plasma peaks at early times and decays through recombination as a function of time.[12] Experiments to determine the exact size and plasma density profile of the laser-induced plasma are currently underway. For this reason, the data is instead presented as a function of Δt, which was the delay time between the laser Q-switch trigger and the time the measurement was taken. With the knowledge that n_e decreases with time, a qualitative comparison of this data to the simulation results was possible.

A plot of the forward transmission coefficient (S_{21}) obtained from this two-port waveguide experiment can be found on Fig. 4a. Some clear similarities arise when comparing this plot to the plot on Fig. 3a. First, the frequency of least transmission (i.e. the resonance frequency) decreases with increasing Δt (decreasing n_e). Also, there appears to be a range of plasma densities and spheroid sizes that lead to resonances in the Ku band of the microwave spectrum. Some differences are also apparent between these two plots, the most notable being the bandwidth of the resonance regions. The much broader bandwidth observed in Fig. 4a could be associated with deviations in the geometry of the plasma from a perfect spheroid as well as gradients in plasma density not taken into account in the simulation.

Fig. 4b is analogous to the plot in Fig. 3b. There are some clear similarities between these two plots as well. The overall variation of S_{21} with Δt (or n_e) is quite similar. In this case, S_{21} reaches a minimum at around $\Delta t = 2.9$ μs. Measurements of peak n_e in laser-induced plasmas conducted by Thiyagarajan and Scharer[16] show

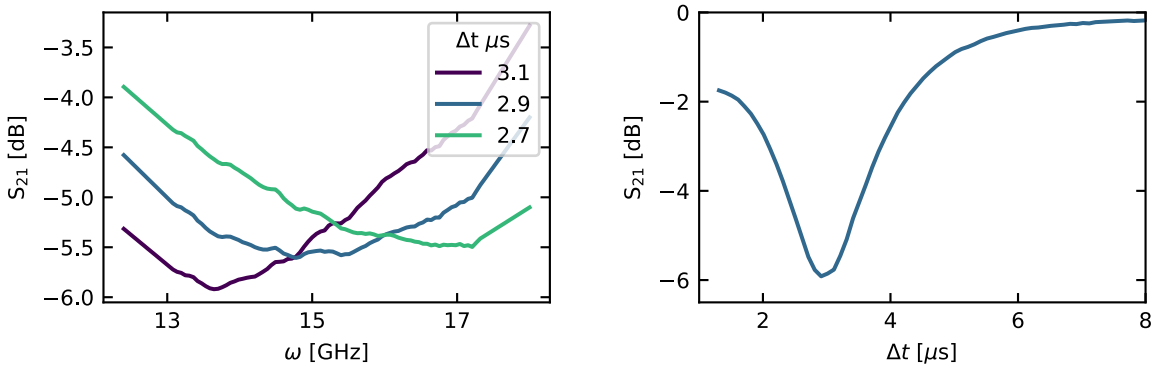

Figure 4. (a) Transmission coefficient vs. frequency for varying plasma density (experiments). (b) Transmission coefficient vs. plasma density at $\omega = 15.2$ GHz (experiments).

that for pressures of 760 Torr and 500 Torr, peak values of n_e approaching those necessary to obtain a resonance at around 15.2 GHz ($n_e \approx 10^{13}$ m^{-3}) occur at $\Delta t \approx 7$ μs and $\Delta t \approx 5$ μs, respectively. Assuming that this trend can be extrapolated to lower pressures, these results support the possibility that a value of $n_e \approx 10^{13}$ m^{-3} can occur at $\Delta t \approx 3$ μs, which provides further support for the existence of the described surface plasmon resonances.

3. SUMMARY

In summary, this paper discussed the potential use of gaseous plasmas as highly-tunable resonators for metamaterial applications. Results were presented from theoretical approximations, FEM simulations, and scattering experiments, all of which provided consistent evidence to support the existence of electric-dipole resonances, or surface plasmon modes, in the described plasma resonators. The tunability and reconfigurability afforded by these resonators could lead to a new class of all-plasma metamaterials with fully three-dimensional structural flexibility in the microwave and low THz regime of the EM spectrum.

ACKNOWLEDGMENTS

This work was supported by the Air Force Office of Scientific Research (AFOSR) under Award No. FA9550-14-10317 through a Multi-University Research Initiative (MURI) grant titled "Plasma-Based Reconfigurable Photonic Crystals and Metamaterials". R. Colón Quiñones gratefully acknowledges the financial support of the National Defense Science and Engineering Graduate Fellowship Program.

REFERENCES

[1] Caloz, C. and Itoh, T., [*Electromagnetic Metamaterials: Transmission Line Theory and Microwave Applications*], John Wiley & Sons, Hoboken, NJ, USA (2005).

[2] Smith, D. R., Pendry, J. B., and Wiltshire, M. C., "Metamaterials and negative refractive index," *Science* **305**(5685), 788–792 (2004).

[3] Zheludev, N. I. and Kivshar, Y. S., "From metamaterials to metadevices," *Nature materials* **11**(11), 917–924 (2012).

[4] Sakai, O. and Tachibana, K., "Plasmas as metamaterials: a review," *Plasma Sources Science and Technology* **21**(1), 013001 (2012).

[5] Lee, D.-S., Sakai, O., and Tachibana, K., "Microplasma-induced deformation of an anomalous response spectrum of electromagnetic waves propagating along periodically perforated metal plates," *Japanese Journal of Applied Physics* **48**(6R), 062004 (2009).

[6] Sakai, O., Shimomura, T., and Tachibana, K., "Negative refractive index designed in a periodic composite of lossy microplasmas and microresonators," *Physics of Plasmas* **17**(12), 123504 (2010).

[7] Singh, P. K., Hopwood, J., and Sonkusale, S., "Metamaterials for remote generation of spatially controllable two dimensional array of microplasma," *Scientific Reports* **4** (2014).

[8] Nakamura, Y., Iwai, A., and Sakai, O., "Nonlinear properties of negative-permittivity microwave plasmas embedded in metamaterial of macroscopic negative permeability," *Plasma Sources Science and Technology* **23**(6), 064009 (2014).

[9] Liu, C.-H., Carrigan, P., Kupczyk, B. J., Xiang, X., Behdad, N., Scharer, J. E., and Booske, J. H., "Metamaterials for rapidly forming large-area distributed plasma discharges for high-power microwave applications," *IEEE Transactions on Plasma Science* **43**(12), 4099–4109 (2015).

[10] Kourtzanidis, K., Pederson, D. M., and Raja, L. L., "Electromagnetic wave energy flow control with a tunable and reconfigurable coupled plasma split-ring resonator metamaterial: A study of basic conditions and configurations," *Journal of Applied Physics* **119**(20), 204904 (2016).

[11] Cohick, Z., Luo, W., Perini, S., Baker, A., Wolfe, D., and Lanagan, M., "A novel, all-dielectric, microwave plasma generator towards development of plasma metamaterials," *Applied Physics Express* **9**(11), 116201 (2016).

[12] Yalçin, Ş., Crosley, D., Smith, G., and Faris, G. W., "Influence of ambient conditions on the laser air spark," *Applied Physics B: Lasers and Optics* **68**(1), 121–130 (1999).

[13] Bohren, C. F. and Huffman, D. R., [*Absorption and Scattering of Light by Small Particles*], John Wiley & Sons, New York, NY, USA (1998).

[14] Zhao, Q., Zhou, J., Zhang, F., and Lippens, D., "Mie resonance-based dielectric metamaterials," *Materials Today* **12**(12), 60–69 (2009).

[15] Mie, G., "Beiträge zur optik trüber medien, speziell kolloidaler metallösungen," *Annalen der physik* **330**(3), 377–445 (1908).

[16] Thiyagarajan, M. and Scharer, J., "Experimental investigation of ultraviolet laser induced plasma density and temperature evolution in air," *Journal of Applied Physics* **104**(1), 013303 (2008).